Studies on Thermal and Spectral Properties of Ho^{3+} : Lithium Borate Glasses

T. Maheswari*, V. Naresh, R. Ramaraghavulu, B. H. Rudramadevi & S. Buddhudu
Department of Physics, Sri Venkateswara University, Tirupati-517502, AP.

Abstract **-We report here on the structural (XRD & Raman), thermal (TG-DTA), dielectric, absorption and emission (Vis & NIR) properties of lithium borate glasses with and without (1 mol %) Ho^{3+} has been prepared using standard melt quenching technique. Based on XRD feature, an amorphous nature of this glass has been confirmed. Raman spectrum has revealed that there exists a transformation of BO_3 triangles into BO_4 tetrahedral with the addition of Li_2O content in the glass composition. Weight loss, glass transition temperature (T_g) have been identified from TG-DTA profiles measured for the lithium borate precursor chemicals mix. From absorption spectrum, absorption and stimulated emission cross-section have been evaluated by applying McCumber's theory and further cross-sectional gain has also been computed for the emissions at 1195 nm (~1.20 µm). On exciting Ho^{3+} glass at (λ_{exci} = 451 nm), two emissions at 556 nm ($^5S_2 \rightarrow {}^5I_8$; *Green*), 655 nm ($^5F5 \rightarrow {}^5I_8$; *Red*) have been obtained. Upon exciting this Ho^{3+} glass with a laser excitation source at 451 nm, an NIR emission at 1199 nm ($^5I_6 \rightarrow {}^5I_8$) has been measured. Dielectric measurements have also been carried for both the undoped host glass and Ho^{3+}doped glass too. Based on those results, ac-conductivity values of these glasses have been evaluated.**

KEY WORDS: Luminescence, Melt quench method and Optical glasses

.

1. INTRODUCTION

Glasses are more advantageous than crystalline materials because of their physical isotropy, absence of grain boundaries and compositional variations [1]. Borate glasses have widely been investigated due to its open like structure. Addition of modifier salt Li_2O to the borate glass composition significantly changes its structure i.e., transforming BO_3 triangles to BO_4 tetrahedral along with an increase in glass thermal stability, humidity withstanding ability associated with chemical durability and transparency from UV to NIR range [2, 3]. Lithium borate glasses find a wide range of technological applications as electro-chemical devices as ionic conductors, optoelectronic devices and fluorescent or luminescent materials depending on the presence of transition metal (or) rare earth ions [4]. When transition metal/ rare earth ions are added in to glassy systems, those could generate different dopant sites by creating strong interaction amongst those ions thus resulting in with an intense optical (absorbance) and spectral (excitation and emission) properties. Among RE^{3+} ions, Ho^{3+} is an interesting ion for spectroscopic studies, because it exhibits several electronic transitions in the visible and NIR and also in Mid- IR regions that are useful for the development of visible and IR solid state lasers. In addition to those uses, glass with Ho^{3+} ion provides an eye-safe potential lasing emission at room temperature with a low threshold action that has attractive applications in atmospheric communication systems. Here, we have investigated the structural, thermal and electrical properties of lithium borate glasses besides optical and VIS-NIR emission for Ho^{3+} as a dopant ion in lithium borate glass matrix.

2. EXPERIMENTAL STUDIES

2.1 Glass sample preparation

By employing a melt quenching technique, glass samples in the following chemical compositions were prepared:

(i) $30Li_2O$-$70B_2O_3$ (host or reference glass)
(ii) 1 mol% Ho_2O_3 : $30Li_2O$-$69B_2O_3$ (Ho^{3+}: LB glass)

Analytical grade (Sigma Aldrich) chemicals of H_3BO_3, Li_2CO_3, and Ho_2O_3 were weighed in 10g batch each separately, thoroughly mixed and finely powdered using an agate mortar and pestle and each of those was collected into porcelain crucibles and heated each of those was put inside in an electric furnace for melting for an hour at 930°C. These melts were quenched in between two smooth surfaced brass plates to obtain glass samples in circular designs with 2-3 cm in diameter and each having a thickness of 0.3 cm. Thus, obtained glassy sample are used for their analysis of different properties.

2.2 Measurements

XRD profiles were recorded on a *Seifert X-ray diffractometer (model 3003TT)* with CuK_α radiation (λ = 1.5406 Å) at 40 KV and 20 mA with a Si detector and $2\theta = 10^o$ and 60^o at the rate of two degrees per minute. A simultaneous measurement of TGA and DTA was carried out on *NetZsch STA 409* at a heating rate of 10^oC/min with N_2 as the purging gas was obtained to correlate these results with FT-IR spectra of the sample recorded on a *Nicolet -5700 FT-IR spectrometer* using KBr pellet technique in the range of 4000-400 cm^{-1}. Electrical conductivity measurements were carried at room temperature over a frequency range of 1 Hz – 1 MHz at an ac voltage strength of 1 V_{rms} on a *Phase Sensitive Multimeter (PSM 1700)* in LCR mode for acquiring the data of real and imaginary parts of complex impedance. The calculation of

conductivity (σ_{ac}), real (ε') and imaginary (ε'') parts of dielectric constant (ε^*), dielectric loss ($tan\delta$) were performed using raw impedance data based on the capacitance, sample dimensions and electrode area. Absorption spectra of glasses were measured on a *Varian-Cary-Win Spectrometer (JASCO V-570).* The emission spectrum of Ho^{3+} doped lithium borate glasses were measured in a steady state mode in a *SPEX Flurolog-3(Model-II) Fluorimeter.* The NIR emission measurement was carried on a Jobin YVON Fluorolog-3 spectrofluorimeter with 450 W Xenon flash lamp as pump source under 451 nm wavelength.

3. RESULTS AND DISCUSSION

3.1 XRD Analysis

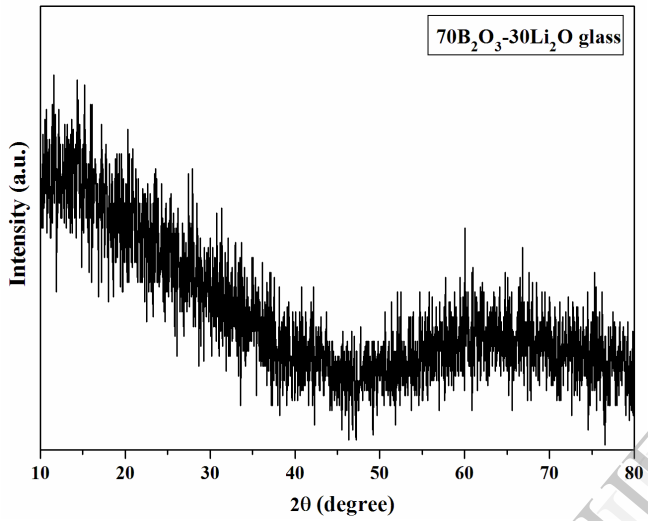

Fig: 1 XRD profile of host B_2O_3- Li_2O glass.

XRD profile of Li_2O-B_2O_3 glass has been shown in Fig.1, profile confirms the amorphous nature of the glass showing a broad diffusion band at lower scattering angles (20^0-30^0).

3.2 FTIR analysis

Fig.2 shows an FTIR spectrum of Li_2O-B_2O_3 glass. The structure of vitreous borate consisting random network of BO_3 triangles transformed into BO_4 network with the inclusion of alkaline metal oxide (Li_2O) [5]. The FTIR spectrum has revealed characteristic peaks located at 685 cm^{-1}, 871 cm^{-1}, 1009 cm^{-1}, 1133 cm^{-1}, 1195 cm^{-1}, 1370 cm^{-1} & 3435 cm^{-1}. In the measured infrared spectral range, the vibrational modes of borate show three regions, the first region at1200-1600 cm^{-1} band is due to an asymmetric stretching of relaxation of the B–O bond of trigonal BO_3 units.

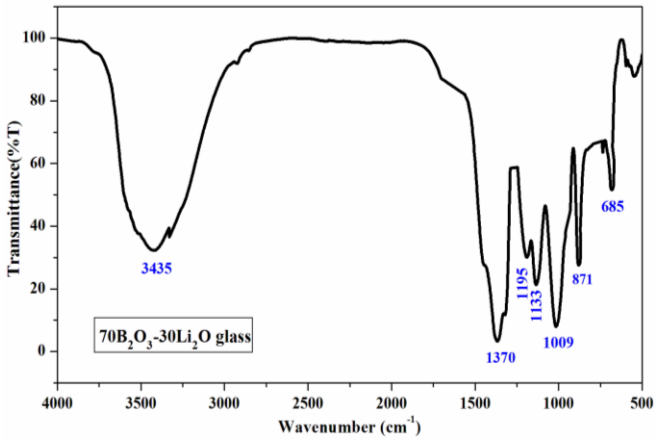

Fig: 2 FTIR spectrum of host B_2O_3- Li_2O glass.

The second region at 800-1200 cm^{-1} is due to the B–O bond stretching of tetrahedral BO_4 units. The third region bands at 600-800 cm-1 is originating from the bending vibrations of B–O–B linkages in borate network [6]. The band at 685cm^{-1} is attributed to characteristic vibrations of Li-O ion. The band at 871 cm^{-1} is arises due to the bending vibrations of B-O-B linkages of BO_3 units, the band at 1009 cm^{-1} is assigned to BO_4 tetrahedral units. The band at 1195 cm^{-1} is assigned to B-O stretching vibrations, the band at 1370 cm^{-1} is assigned to planar BO_3 group. The band at 3435 cm^{-1} is assigned to Hydrogen bonding due to O-H stretching vibration [7].

3.3 Thermal (TG-DTA) Analysis

The thermal behavior of the Li_2O-B_2O_3 precursor chemical mix has been shown in Fig.3.

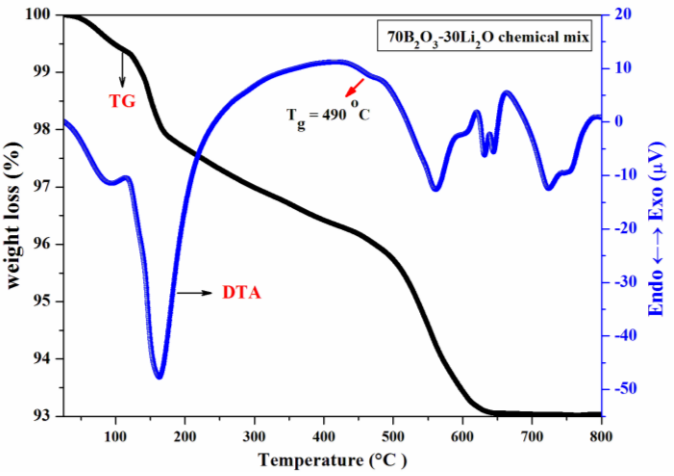

Fig: 3 TG & DTA profiles of host B_2O_3- Li_2O precursor chemical mix.

The TG profile shows that the weight loss is taking place in a multi step process in the temperature range of 30°C–800°C. The initial weight loss takes place between 30°C–175°C due to the decomposition of the organic compounds that were added while grinding raw chemicals to obtain homogeneity and water present in the sample which is about 2%. A weight loss of 1.5% has been noticed in the temperature range of 176°C–465°C due to a phase change of H_3BO_3 in to B_2O_3. Final weight loss of 2.5 % has been identified in the temperature range of

460°C–610°C, that could be due to decomposition of Li_2CO_3 to Li_2O and thereafter no appreciable weight loss has been noticed in the sample due to formation of a stable compound [7]. The DTA profile of host precursor chemicals mix shows an endothermic peak at 162^0 C which is attributed to the short range order and partial melting of small percentage of impurity phase phase change of H_3BO_3 to B_2O_3. The glass transition temperature (Tg) has been noticed at 490°C [7, 8].

3.4 Absorption, stimulated emission cross-section and gain spectra characteristics

Fig.4 (a) shows the Visible-NIR absorption spectra of Li_2O-B_2O (host) and Ho^{3+}: Li_2O-B_2O_3 glasses. In the reference Li_2O-B_2O glass, the absorption edge lies in the UV- region and no absorption peak has been observed. When Ho^{3+} ion is doped in lithium borate glass some peaks attributed to *4f-4f* electronic transitions of Ho^{3+} ions have been observed along with a shift in the absorption edge towards lower energy side. This shift in absorption edge could be due to increase in non-bridging oxygens (NBOs).

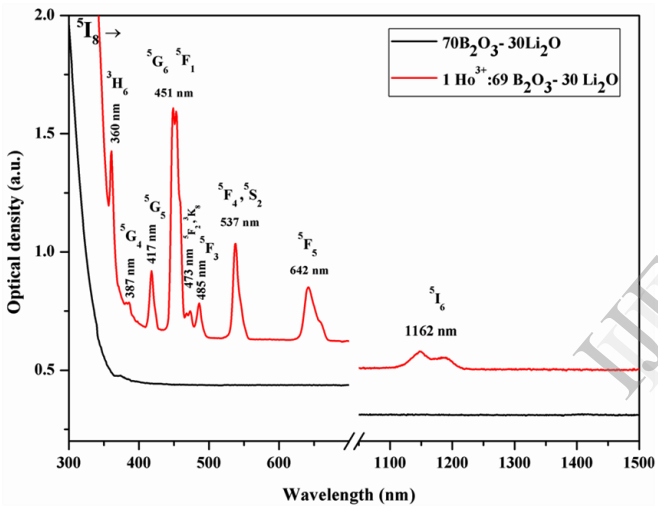

Fig: 4(a) Absorption spectra of both B_2O_3- Li_2O and Ho^{3+}:B_2O_3- Li_2O glasses.

The optical absorption spectrum Ho^{3+}glass exhibits bands at 360nm, 387nm, 417nm, 451nm, 473nm, 485nm, 537nm, 642nm, 1162nm which correspond to the electronic transitions of $^5I_8 \rightarrow {}^3H_6$, $^5I_8 \rightarrow {}^5G_4$, $^5I_8 \rightarrow {}^5G_5$, $^5I_8 \rightarrow {}^5G_6$,$^5F_1$; $^5I_8 \rightarrow {}^5F_2$,$^3K_8$; $^5I_8 \rightarrow {}^5F_3$, $^5I_8 \rightarrow {}^5F_4$, $^5S_2$; $^5I_8 \rightarrow {}^5F_5$ and $^5I_8 \rightarrow {}^5I_6$, respectively [9]. Among these, the transition $^5I_8 \rightarrow {}^5G_6$ (451 nm) is hypersensitive in nature obeying laporte's selection rulesΔS = 0, $\Delta J = 2$ and $\Delta L = 2$. In Fig.4 (b), the absorption and stimulated emission cross-sections obtained for lithium borate glass doped with 1 mol % of Ho^{3+} at 1.20 µm is shown. Absorption cross-section (σ_{abs}) is determined from absorption spectrum data by employing Lambert-Beer Law formula given below [10]:

$$\sigma_{abs} = \frac{2.303 \log\left(I_0 / I\right)}{Nl} \qquad \ldots (1)$$

where N is the concentration of the rare earth ion, l is the thickness of the sample, (I_o/I) is the absorption intensity, I_o and I are the intensities of incident and transmitted light .

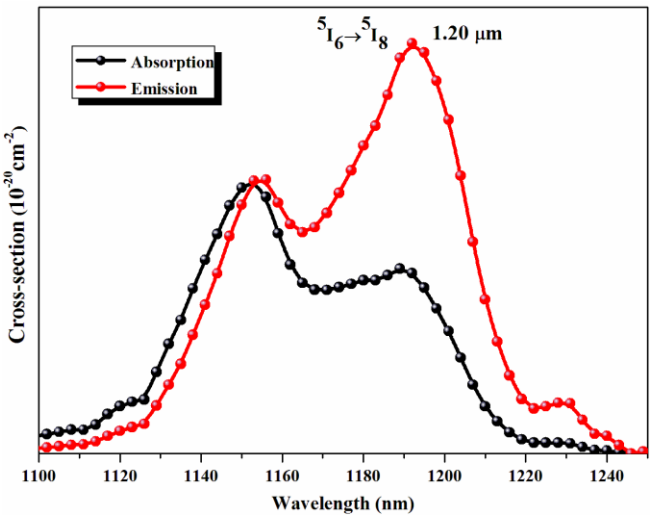

Fig: 4(b) Absorption & stimulated emission cross-section spectra of Ho^{3+}:B_2O_3- Li_2O glass at ~1.20 µm emission.

According to McCumber's theory, stimulated emission cross-section (σ_{emi}) of Ho^{3+} $^5I_6$, $^5I_7 \rightarrow {}^5I_8$ transition is derived from $^5I_8 \rightarrow {}^5I_6$, $^5I_7$ transition of the absorption cross-section (σ_{abs}) [11]:

$$\sigma_{emi}(\lambda) = \sigma_{abs}(\lambda) \exp\left[\left(\varepsilon - h\nu\right) / kT\right] \qquad \ldots (2)$$

where ν is the photon frequency, k is the Boltzmann constant, ε is the free energy required to excite Ho^{3+} ion from ground state to excited state at temperature T, σ_{abs} is the absorption cross-section. A close overlap between the absorption and emission cross-section spectra suggests re-absorption of the emitted radiations of Ho^{3+} ions and is re-emitted resulting in spectral broadening, which is normally observed in a three level system.

Fig.4 (c) shows the gain spectra as a function of population inversion rate (β). The gain coefficient is calculated from the absorption cross-section data using the expression given below as:

$$G(\lambda) = N[\beta\sigma_{emi}(\lambda) - (1-\beta)\sigma_{abs}(\lambda)] \qquad \ldots (3)$$

where N ($N = N_1+N_2$) is the concentration of the Ho^{3+} ion, β is the population inversion rate ($= N_2/N_1$) which is dependent on the pump energy-density and its value falls into the region 0 to 1.

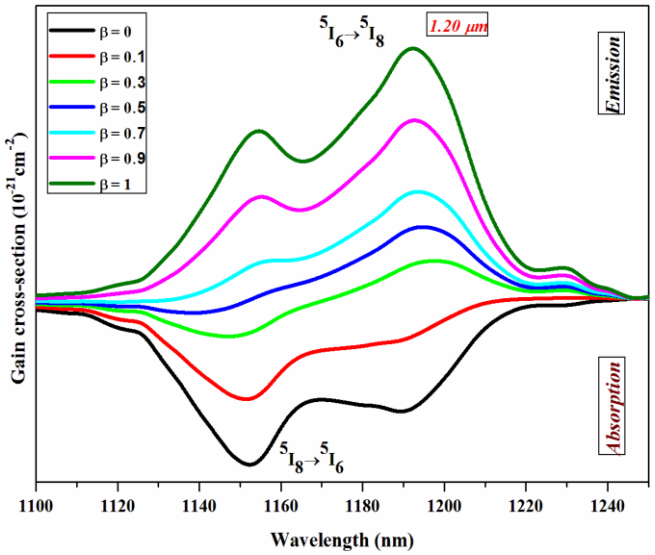

Fig:4(c) Gain cross-section as function of population inversion parameter β

From the Fig. 4 (c), it is observed that when the population inversion rate (β) takes the values from 0 to 1, the spectra evolved depicts like absorption cross-section spectra and as the values of β increases from 1 to 1, gain achieves maxima in the positive axis attributed to 1.20μm resembling as NIR emission spectra of Ho^{3+}. Generally, this type of characteristic phenomenon is exhibited by quasi three level lasers.

3.5 Photoluminescence (Vis-NIR) spectral properties of Ho^{3+}:Li_2O-B_2O_3 glass

Fig.5 (a) shows the excitation spectrum of Ho^{3+} doped lithium borate glass by monitoring with a strong emission band located at 548 nm (green). The spectrum has displayed three excitation bands that are assigned to the electronic transitions of $^5I_8 \rightarrow {}^5G_5$, $^3G_5$ (418 nm), $^5I_8 \rightarrow {}^5G_6$ (451 nm), $^5I_8 \rightarrow {}^5F_3$ (486 nm) respectively. Of these, the prominent transition at 451 nm ($^5I_8 \rightarrow {}^5G_6$) has been used for recording the emission spectrum of Ho^{3+} doped glass in the visible wavelength region [12, 13].

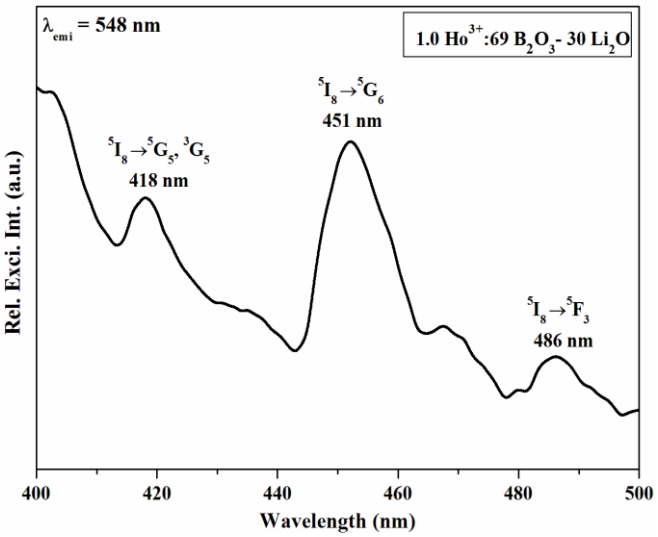

Fig: 5(a) Excitation spectrum of Ho^{3+}:B_2O_3- Li_2O glass.

The photoluminescence (Vis and NIR emission) spectra of Ho^{3+}: lithium borate glass is shown in Figs.5 (b & c).

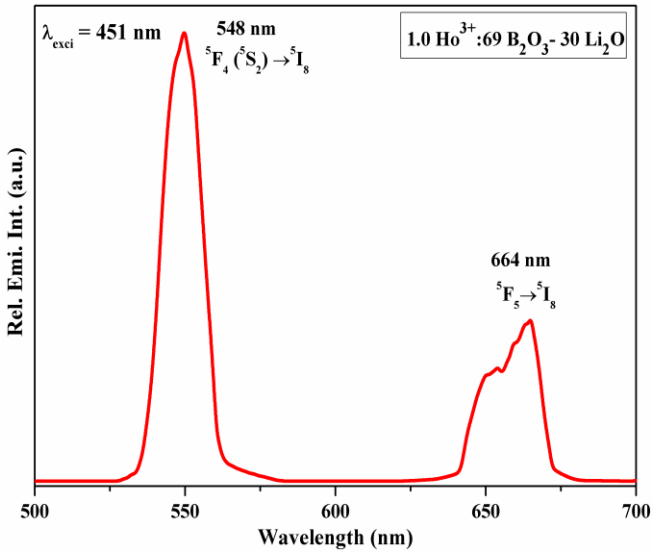

Fig: 5(b) Vis-emission spectrum of Ho^{3+}:B_2O_3-Li_2O glass.

From excitation spectrum, the band at 451 nm has been chosen to record the emission spectrum of Ho^{3+} doped lithium borate glass as shown in Fig. 5 (b). Ho^{3+} ions are excited to higher energy levels from where they decay non-radiatively to $^5F_4$ and $^5F_5$ states and subsequently relax to the ground state $^5I_8$ with emissions at 548nm (*green*) and 664 nm (*red*) corresponding to the electronic transitions $^5F_4 \rightarrow {}^5I_8$ and $^5F_5 \rightarrow {}^5I_8$ respectively [12-14].

In Fig. 5 (c), NIR emission spectrum of Ho^{3+} doped lithium borate glass has been shown with an excitation 451 nm. In the emission spectra, an intense emission band at 1.20 μm ($^5I_6 \rightarrow {}^5I_8$) associated with a weak band at 1.37μm ($^5F_4$ ($^5S_2$)$\rightarrow {}^5I_5$) have been observed [15, 16].

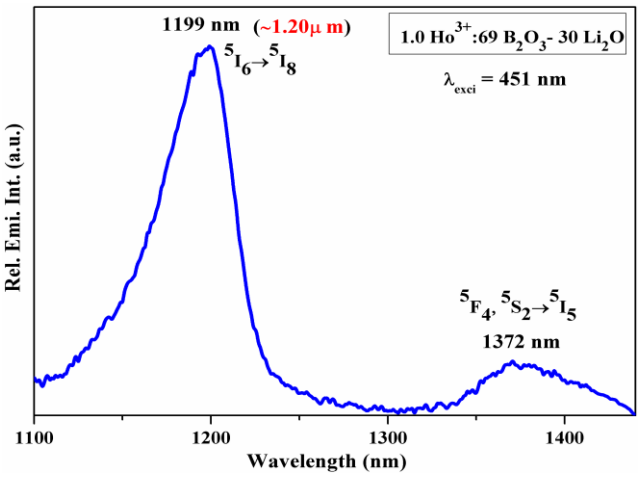

Fig: 5(c) NIR-emission spectrum of Ho^{3+}:B_2O_3-Li_2O glass.

The energy level scheme of the $1Ho^{3+}$:$30Li_2O$-$69B_2O_3$ glass shown in the Fig. 6 explains emission process involved in the visible-NIR photoluminescence of Ho^{3+} glass.

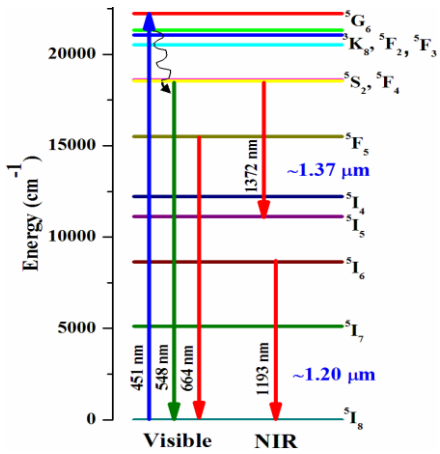

Fig: 6 Energy level scheme of Ho^{3+} ion.

3.6 Dielectric (ε′ & tanδ) and a.c conductivity analysis

When dielectric material has been introduced in an a.c electric field, there will be a phase log between the applied field and the response of the system. This is due to the losses associated with the presence of polarizable entities in the dielectric or due to inertial effects [17]. In the dielectric studies, the complex permittivity of the system is calculated using the impedance data:

$$\varepsilon^* = \frac{1}{\left(j\omega C_\circ Z^*\right)} = \varepsilon' - j\varepsilon'' \qquad \ldots (4)$$

where Z^* is the complex impedance, C_o is the capacitance of free medium. The real part of permittivity (dielectric constant) ε′ represents the polarizability of the material (or energy stored in a material), while the imaginary part (dielectric loss) ε" represents the energy loss due to polarization and ionic conduction.

The dielectric constant (ε′) and dielectric loss factor are calculated using the formulae:

$$\varepsilon' = \frac{Cd}{\varepsilon_\circ A} \qquad \ldots (5)$$

and

$$\varepsilon'' = \varepsilon' \tan\delta \qquad \ldots (6)$$

Where C is the capacitance of the glass sample, ε_o is the permittivity of the free space (8.85×10^{-12} F/m and A is the cross-sectional area of electrode. where tan δ is the loss tangent. The ac conductivity of the sample (σ_{ac}) was determined from dielectric parameters using the relation:

$$\sigma_{ac} = \omega \varepsilon_\circ \varepsilon'' \qquad \ldots (7)$$

where ω is an angular frequency.

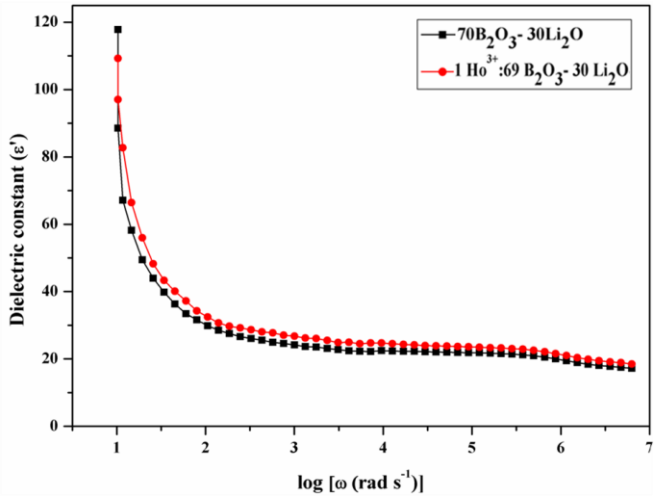

Fig: 7(a) Dielectric constant (ε') values as function of log (ω) for B_2O_3- Li_2O and Ho^{3+}:B_2O_3- Li_2O glasses.

In Fig. 7 (a), Dielectric constant (ε') as a function of log (ω) at the room temperature for Lithium borate glasses with and without Ho^{3+} are shown. From this figure it has been observed that the dielectric constant (ε′(ω)) value decreases with an increase in frequency and reaches to a minimum value without any further decrease from 1Hz to 1MHz for the glasses studied. The dielectric constant describes the polarizing performance of a material in the presence of an applied electric field. At lower frequencies, due to absence of net polarization, the ions get accumulated at the electrode-electrolyte interface forming a space charge region causing immobilization of charges leading to high ε' value. As frequency increases, the periodic reversal of electric field occurs so fast that no excess ions accumulate in the electric field direction and hence, the dielectric constant is lowered by weakening of ion-ion interaction in the dipoles as a result their contribution to the polarization would be reduced [18, 19].

Loss tangent or dielectric loss factor (tanδ) as a function of log (ω) at room temperature for Lithium borate glasses with and without Ho^{3+} is shown in Fig.7 (b). Both the glasses with and without dopant (Ho^{3+}) ion have exhibited same decreasing trend with increasing of frequency because, when the electric field is applied the dipoles rotate to align themselves in the field direction. As the time passes, the electric field reverses its direction the dipoles also rotate again to remain aligned in the direction of electric field with the correct polarity. As it rotates, energy is lost through the generation of heat (friction). More energy is being dissipated through motion therefore less energy is available to propagate the dipoles.

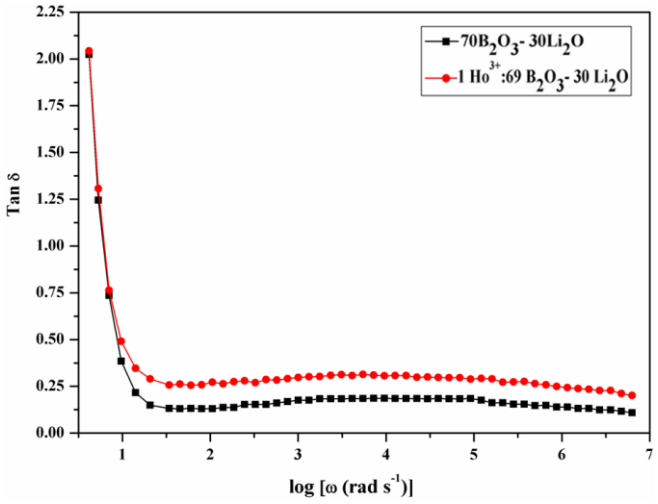

Fig: 7(b) Dielectric loss factor (tanδ) values as function of log (ω) for B_2O_3- Li_2O and Ho^{3+}:B_2O_3- Li_2O glasses.

. The dielectric loss tangent has high dispersion at low frequency, which decrease gradually as frequency increases due to less contribution of ions in the direction of applied electric field [19, 20].

The frequency dependent mechanism for the present glass system is analyzed on the basis of Jonscher universal power law [21]:

$$\sigma(\omega) = \sigma_{dc} + A\omega^{S} \qquad 0 < s < 1 \qquad \ldots (8)$$

Where σ_{dc} is the dc conductivity of the samples, $A\left(= \sigma_{dc} / \omega_P^S\right)$ is temperature dependent constant, $\omega = 2\pi f$ is the angular frequency of the applied field and *s* is the power law exponent in the range $0 < s < 1$, represents the degree of interaction between the mobile ions and it can be measured by taking slope of $\log \sigma_{ac}(\omega)$ versus $\log \omega$ for the curves . From the Fig. 7 (c), it is observed that the two profiles of Lithium borate glass with and without dopant Ho^{3+} ion have shown same trend with nearly flat portion at lower frequencies and at higher frequencies conductivity exhibits dispersion which increases nearly following power law relation:

$$\sigma(\omega) = A\omega^{S} \; s<1 \qquad \ldots (9)$$

From the ac-conductivity profile it is noticed that the conductivity due to Ho^{3+} doped lithium borate glass has been decreased when compared to lithium borate glass. Such decrease in conductivity could be due to introduction of high density of rare earth (Ho^{3+}) ion in high concentrations (1 mol %) polymerizes the glass network by decreasing the molar volume as a result number of path ways available for Li^+ ions conduction decreases. The other reason for decrease in mobility of Li^+ ions is due to their bonding with the available non-bridging oxygens and also could be due to formation of the quasi-molecular complex (clusters) of rare earth ions with the glassy matrix [22-24].

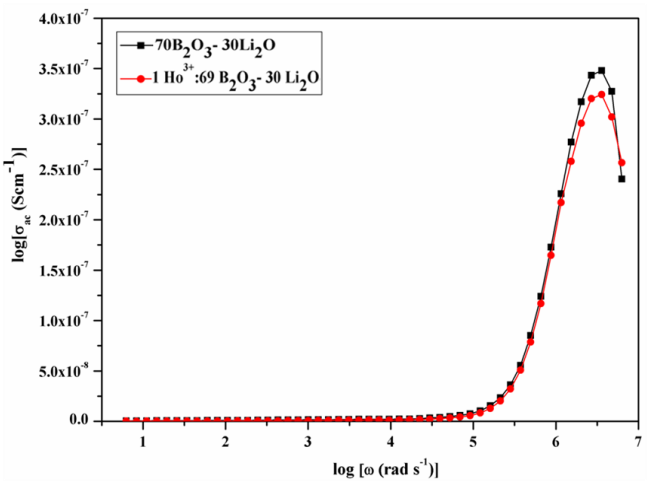

Fig: 7(c) Ac-conductivities (log σ_{ac}) as function of log (ω) for B_2O_3- Li_2O and Ho^{3+} :B_2O_3- Li_2O glasses.

The analysis of frequency dependent electrical properties show that the value of dielectric constant (ε') decreases with increasing frequency and accordingly increases in conductivity (σ_{ac}) has been explained.

4. CONCLUSION

In summary, it is concluded that we have successfully developed a couple of transparent optical glasses in the composition of 1 Ho^{3+}:$69B_2O_3$-$30Li_2O$ and also a reference glass of $70B_2O_3$-$30Li_2O$ by using a standard melt quench technique. The optical absorption, XRD, FT-IR and TG-DTA profiles of the host lithium borate glass have been undertaken to analyze its structural and thermal properties. From optical absorption spectra it is noticed that the prepared lithium borate glass with and without Ho^{3+} ion posses good UV transmission ability. From the dielectric (ε′ & tanδ) properties, it is observed that both glasses have exhibited same trend of decreasing dielectric constant and dielectric loss with an increase in the frequency. Because the dipoles are no longer able to orient rapidly so that their oscillations begin to lag behind those of electric field in the glasses studied. Ac conductivity value has been found to be increasing with an increase in the frequency for both the glasses. But due to presence of Ho^{3+} ion in the lithium borate glass, its conductivity has been found decreased compared with the reference glass. The optical characterizations based on the measurement of absorption, emission bands have been observed for the reference and Ho^{3+} ion doped glass in Visible and NIR regions. Emission levels cross-sections and their gain at ~1.20 µm of Ho^{3+}. An intense green emission ($^5F_4 \rightarrow {}^5I_8$; 14 µm) and a week red emission ($^5F_5 \rightarrow {}^5I_8$; 0.66 µm) and also a couple of NIR emission bands ($^5I_6 \rightarrow {}^5I_8$; ~1.20 µm and $^5F_4$, $^5S_2$) $\rightarrow {}^5I_5$; 1.37 µm) of Ho^{3+} doped lithium borate glass has been noticed upon exciting at 451 nm. Our results provide an opportunity to suggest that these glasses could significant potentiality with an encouraging importance in the progress and development of luminescent optical systems.

REFERENCES

1. B. V. R. Chowdari & Zhou Rong, Study of the fluorinated lithium borate glasses, Solid State Ionics 78 (1995) 133-142.
2 R. L. Mozzi & B. E. Warren, The structure of vitreous boron oxide, J. Appl. Crystallogr. 3 (1970) 251.
3. M. Irion and M. Couzi, A. Levasseur, J. C. Brethous, J. M. Reau & P. Hagenmuller, An infrared and Raman study of new lonic-conductor lithium glasses, J. Solid State Chem. 31(1980) 285.
4. R. Balaji Rao, A. R. Gerhardt & N. Veeraiah, Spectroscopic characterization, conductivity and relaxation anomalies in the $Li_2O–MgO–B_2O_3$ glass system: Effect of nickel ions, J. Phys. Chem. Solids 69 (2008) 2813.
5. J. Krogh-Moe, The structure of vitreous and liquid boron oxide, J. Non-Cryst. Solids, 1 (1969) 269.
6. J. Coelho, C. Freire, N. Sooraj Hussain, Structural studies of lead lithium borate glasses doped with silver oxide, Spectrochim. Acta A 86 (2012) 392.
7. V. Naresh & S. Buddhudu, Structural, thermal, dielectric and ac conductivity properties of lithium fluoro-borate optical glasses, Ceram. Int. 38 (2012) 2325.
8. R.M. Mohamed, Effect of irradiation on differential thermal properties and crystallization behavior of some lithium borate glasses, Nucl. Instrum. Methods B, 179 (2001) 230.
9. W. T. Carnall, P. R. Fields, and R. Rajnak, Electronic energy levels in the trivalent lanthanide aquo ions, J. Chem. Phys. 49 (1964) 4424-4442.
10. D. Rajesh, Y. C. Ratnakaram, A. Balakrishna, Er3+-doped strontium lithium bismuth borate glasses for broadband 1.5 μm emission – Structural and optical properties, J. Alloy Compd, 563 (2013) 22.
11. D. E. McCumber, Theory of Phonon-Terminated Optical Masers, Phys. Rev. B 134 (1964) A299.
12. N. Sooraj Hussain, N. Ali, A.G. Dias, M.A. Lopes, J.D. Santos & S. Buddhudu, Absorption and emission properties of Ho3+ doped lead–zinc–borate glasses,Thin Solid Films 515 (2006) 318.
13. T. Suhasini, B.C. Jamalaiah, T. Chengaiah, J. SureshKumar & L. RamaMoorthy, An investigation on visible luminescence of Ho3+ activated LBTAF glasses, Physica B 407 (2012) 523.
14. B. Karmakar, IRRS, UV-Vis-NIR absorption and photoluminescence upconversion in Ho3+-doped oxyfluorophosphate glasses, J. Solid State Chem., 178 (2005) 2663.
15. B.J. CHEN, L.F. SHEN, E.Y.B. PUN, H. LIN, 1.2 MM NEAR-INFRARED EMISSION AND GAIN ANTICIPATION IN HO^{3+} DOPED HEAVY-METAL GALLATE GLASSES, OPT. COMMUN. 284 (2011) 5705.
16. M. Ichikawa, Y. Ishikawa, T. Wakasugi, Kohei Kadono, Mid-infrared emissions from Ho3+ in Ga_2S_3-GeS_2-Sb_2S_3 glass, J. Lumin, 132 (2012) 784.
17. H. K. Patel & S. W. Martin, Fast ionic conduction in $Na_2S+B_2S_3$ glasses: Compositional contributions to non exponentiality in conductivity relaxation in the extreme low-alkali-metal limit, Phys. Rev. B, 45 (1992) 10292.
18. A.K. Jonscher, Analysis of the alternating current properties of ionic conductors, J. Mater. Sci., 13 (1978) 553-562.
19. A. K. Jonscher, Dielectric Relaxation in Solids, Chelsea Dielectric Press, London, (1983).
20. J. R. Macdonald (Ed.), Impedance Spectroscopy – Emphasizing Solid Materials and Systems, John Wiley & Sons, New York, (1987).
21. A. K. Jonscher, The 'universal' dielectric response, Nature 267 (1977) 673-679.
22. G. B. Devidas, T. Sankarappa, M. Prashant Kumar & Santosh Kumar, AC conductivity in rare earth ions doped vanadophosphate glasses, J. Mater. Sci. 43 (2008) 4856.
23. M. M. Elkholy, Dc and ac electrical conductivity of rare earths doped tellurite glasses, Phys. Chem. Glasses 42 (2001) 49.
24. M. H. Shaaban, A. A. Ali & L. K. El-Nimr, The AC Conductivity of tellurite glasses dopped with Ho_2O_3, Mater. Chem. Phys., 96 (2006) 433.